5′-Iodotubercidin represses *insulinoma-associated-1* expression, decreases cAMP levels, and suppresses human neuroblastoma cell growth

Chiachen Chen[‡], **Mary Beth Breslin**[§1], **Jessie J. Guidry**[¶], and ⓘ **Michael S. Lan**[‡§2]

From the Department of [‡]*Genetics,* [§]*Pediatrics, and* [¶]*Biochemistry and Molecular Biology and the LSUHSC Proteomics Core Facility, Louisiana State University Health Sciences Center, New Orleans, Louisiana 70112*

Edited by Xiao-Fan Wang

Insulinoma-associated-1 (INSM1) is a key protein functioning as a transcriptional repressor in neuroendocrine differentiation and is activated by N-Myc in human neuroblastoma (NB). INSM1 modulates the phosphoinositide 3-kinase (PI3K)-AKT Ser/Thr kinase (AKT)-glycogen synthase kinase 3β (GSK3β) signaling pathway through a positive-feedback loop, resulting in N-Myc stabilization. Accordingly, INSM1 has emerged as a critical player closely associated with N-Myc in facilitating NB cell growth. Here, an INSM1 promoter-driven luciferase-based screen revealed that the compound 5′-iodotubercidin suppresses adenosine kinase (ADK), an energy pathway enzyme, and also INSM1 expression and NB tumor growth. Next, we sought to dissect how the ADK pathway contributes to NB tumor cell growth in the context of INSM1 expression. We also found that 5′-iodotubercidin inhibits INSM1 expression and induces an intra- and extracellular adenosine imbalance. The adenosine imbalance, which triggers adenosine receptor-3 signaling that decreases cAMP levels and AKT phosphorylation and enhances GSK3β activity. We further observed that GSK3β then phosphorylates β-catenin and promotes the cytoplasmic proteasomal degradation pathway. 5′-Iodotubercidin treatment and INSM1 inhibition suppressed extracellular signal-regulated kinase 1/2 (ERK1/2) activity and the AKT signaling pathways required for NB cell proliferation. The 5′-iodotubercidin treatment also suppressed β-catenin, lymphoid enhancer–binding factor 1 (LEF-1), cyclin D1, N-Myc, and INSM1 levels, ultimately leading to apoptosis via caspase-3 and p53 activation. The identification of the signaling pathways that control the proliferation of aggressive NB reported here suggests new options for combination treatments of NB patients.

Childhood tumors of the nervous system are derived from granule neuron precursors and precursors of sympatho-adrenal lineage (1, 2). Insulinoma-associated-1 (INSM1)[3] is a crucial component of the transcriptional network that controls the differentiation of sympatho-adrenal lineage for adrenal gland (3). Farkas *et al.* (4) revealed that the induction of Insm1 expression in the developing brain correlates with areas of the brain in which neurogenesis occurs, such as the external granule cell layer of the developing cerebellum, the dentate gyrus of the postnatal hippocampus, the ventricular zone, and in particular, the subventricular zone of the neocortex. Amplification of *N-Myc* gene is a predominant marker for aggressive neuroblastoma (NB) and correlates with poor prognosis (5–7). N-Myc is also the primary executor of Sonic Hedgehog (Shh) signaling. Both Shh and N-Myc are important signals to mediate normal neuronal development. *N-Myc* amplification in NB leads to overexpression at both the N-Myc mRNA and protein levels (8–11). A recent finding uncovered that Shh induces INSM1, a neuroendocrine (NE) factor in NB via the N-Myc activation pathway (12). Strong evidence supports that the cross-talk of Shh, N-Myc, and INSM1 plays a crucial role in NB cell proliferation. Shh signaling induces INSM1 and promotes NB cell growth. *INSM1* is a newly discovered target gene activated by N-Myc. Therefore, the current study focuses on INSM1 to explore novel signaling pathways underlying NB growth. Human NB is the most common childhood extracranial tumor arising from the sympathetic nervous system (1) and amplification of N-Myc occurs in roughly 30% of NB patients and strongly correlates with advanced stage disease and poor outcome (5–7). This study aims to find a new drug for the treatment of aggressive NB tumors. An INSM1 promoter-driven luciferase screening platform was used and identified

---

[1] Present address: Southwest Shadow, SWCTA-7050 W. Shelbourne Ave., Las Vegas, NV 89113.

[2] To whom correspondence should be addressed: Louisiana State University Health Sciences Center, 533 Bolivar St., CSRB Box 6–16 New Orleans, LA 70112. Tel.: 504-568-2437; Fax: 504-568-8500; E-mail: mlan@lsuhsc.edu.

[3] The abbreviations used are: INSM1, insulinoma-associated-1; NB, neuroblastoma; Shh, Sonic Hedgehog; NE, neuroendocrine; ADKi, adenosine kinase inhibitor; ADA, adenosine deaminase; AR, adenosine receptor; 5′-IT, 5′-iodotubercidin; ERK1/2, extracellular signal-regulated protein kinases 1 and 2; CPA, N^6-cyclopentyladenosine; RA, retinoic acid; DAPT, N-[N-(3,5-difluorophenacetyl)-L-alanyl]-S-phenylglycine t-butyl ester; TSA, trichostatin A; AKT, RAC-α-serine/threonine protein kinase; PI3K, phosphatidylinositol-4,5-bisphosphate 3-kinase; GSK3β, glycogen synthase kinase 3β; MTS, 3-(4,5-dimethyl-2-yl)-5-(3-carboxymethoxyphenyl)-2-(4-sulfophenyl)-2H-tetrazolium; Luc2, luciferase 2; NT, nucleoside transporter; KD, knockdown; RP-HPLC, reverse phase-high performance liquid chromatography; LEF-1, lymphoid enhancer–binding factor 1; AMPK, AMP-activated protein kinase; GAPDH, glyceraldehyde-3-phosphate dehydrogenase; ARA$_3$, adenosine receptor-3.
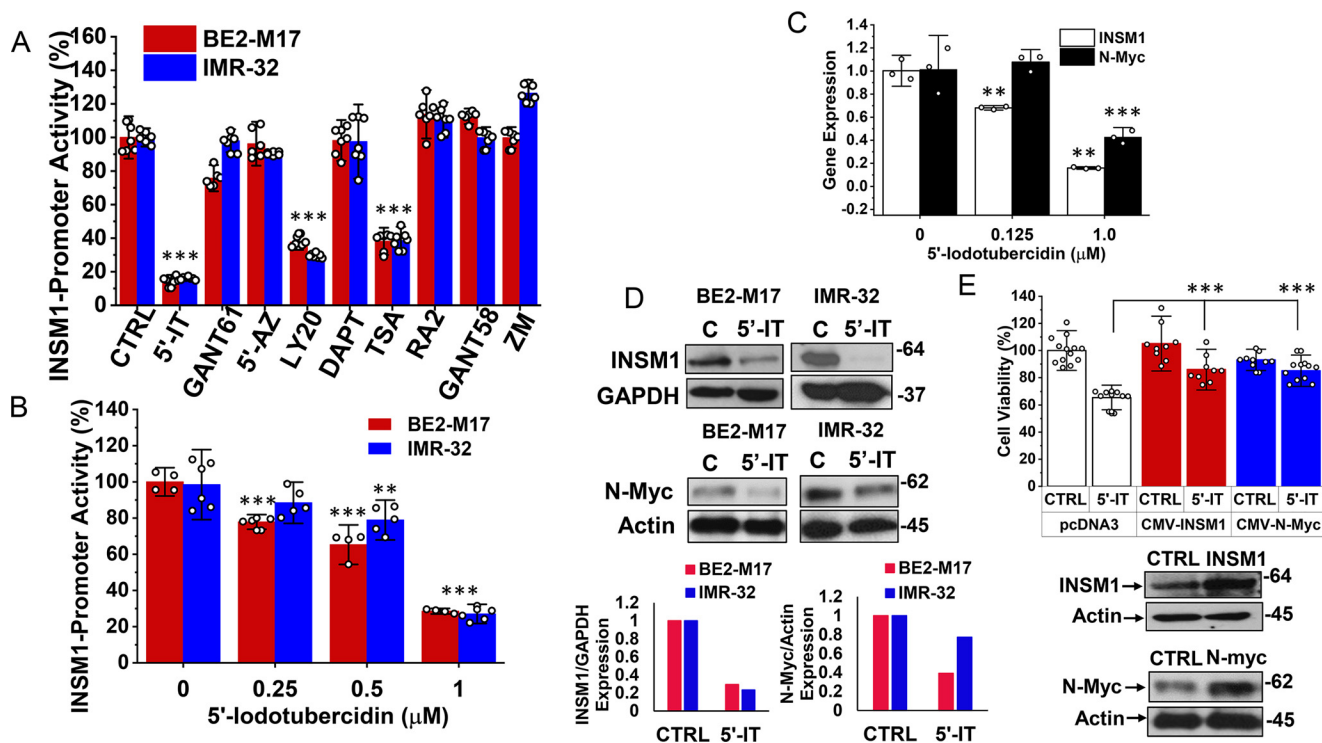

Figure 1. 5′-IT inhibits INSM1 and N-Myc in BE2-M17 and IMR-32 NB cells. *A,* pGL4.18-INSM1p-Luc2 vector transfected BE2-M17 (maintained in G418, 300 μg/ml) or IMR-32 (maintained in G418, 200 μg/ml) stable cell line was seeded in a 96-well plate for compound treatment. DMSO was used as solvent control (100%). *A,* cells were treated with 1 μM 5′-IT, 20 μM GANT61, 10 μM 5′-AZ (5-aza-2-deoxycytidine), 20 μM LY294002, 10 μM DAPT, 0.4 μM TSA, 2 μM RA, 20 μM GANT58, or 10 μM ZM336372 for 48 h and subjected to luciferase activity assay relative to DMSO control. Data represent mean ± S.D. ***, $p \leq 0.001$ ($n = 6–8$/group). *B,* a 5′-IT dose-response assay was performed on INSM1 promoter activity for 24 h. Data represent mean ± S.D. **, $p \leq 0.01$; ***, $p \leq 0.001$ ($n = 4–6$/group). *C* and *D,* pGL4.18-INSM1-Luc2 transfected BE2-M17 or IMR-32 stable cells were treated with 5′-IT for 72 h. INSM1 or N-Myc expression was detected using real-time RT-PCR and Western blot analysis. GAPDH or actin was used as loading control. Data represent mean ± S.D. **, $p \leq 0.01$; ***, $p \leq 0.001$ ($n = 3$/group). *E,* BE2-M17 cells were transfected with CMV-INSM1, CMV-N-Myc, or pcDNA3 control vector (100 ng/well) using Lipofectamine 2000 for 48 h and treated with or without 5′-IT (1 μM) for 48 h before MTS assay. Data represent mean ± S.D. ***, $p \leq 0.001$ ($n = 9–13$/group). Overexpression of INSM1 or N-Myc as compared with the endogenous INSM1 or N-Myc is shown by Western blotting analyses.

an inhibitor (5′-iodotubercidin, 5′-IT) of adenosine kinase (ADKi). Treatment of NB with 5′-IT down-regulates INSM1 and inhibits NB cell growth. ADKi inhibits adenosine kinase (ADK) signaling and modulates intra- and extracellular adenosine metabolism, which is critical for NB tumor cell growth.

The primary function of ADK is to regulate intracellular/extracellular adenine nucleotide pools mediated through the adenosine receptor (AR), inosine formation, and/or energy-sensing AMP-activated protein kinase (AMPK) signaling pathways. The mechanistic connection between ADKi and neuroblastoma (NB) tumor cell growth remains unclear. In this study, for the first time we demonstrate that 5′-iodotubercidin (5′-IT) blockage of the adenosine kinase (ADK) pathway inhibits INSM1 expression and promotes the AR signaling pathway contributing to the suppression of NB tumor cell viability. 5′-IT increases the intra- and extracellular adenosine levels that triggers the ARA₃ signaling pathway resulting in the inhibition of intracellular cAMP affecting NB tumor cell growth. 5′-IT modulates cAMP via ARA₃ leading to the activation of GSK3β and β-catenin phosphorylation. Additionally, 5′-IT and INSM1 suppression inhibit ERK1/2 phosphorylation. Inhibition of these two signaling pathways resulted in LEF-1, INSM1, N-Myc, and cyclin D1 down-regulation while activating caspase-3 and p53 to promote apoptosis.

Results

Drug screen of NB using INSM1 promoter-driven luciferase assay

In a previous study, multiple signaling pathways were identified that regulate NB tumor cell growth in the context of two oncogenic proteins, N-Myc and INSM1 (12). Thus, stable cell lines in BE2-M17 or IMR-32 containing an INSM1 promoter-driven luciferase reporter gene was developed. Using this luciferase-based screening platform, we screened nine compounds previously selected for INSM1 functional study in our laboratory with a medium range of concentrations *versus* DMSO control (Fig. 1A). The screening results showed only marginal effects on INSM1 promoter activity when treated with retinoic acid (RA, 2 μM), GANT61 (20 μM), 5-aza-2-deoxycytidine (5′-AZ) (10 μM), DAPT (10 μM), GANT58 (20 μM), or ZM336372 (10 μM). LY294002 (20 μM) or trichostatin (TSA, 0.4 μM), suppresses ~60% of the INSM1 promoter activity, whereas 5′-IT (1 μM) suppresses the INSM1 promoter activity over 80%. LY294002 is a strong nonselective inhibitor of phosphoinositide 3-kinase (PI3K) (13). TSA selectively inhibits the class I and II mammalian histone deacetylase (HDAC) family of enzymes and cell cycle progression (14). 5′-IT is an adenosine kinase (ADK) inhibitor that displays potent suppressive effects on INSM1 promoter activity. A 5′-IT dose-response study on
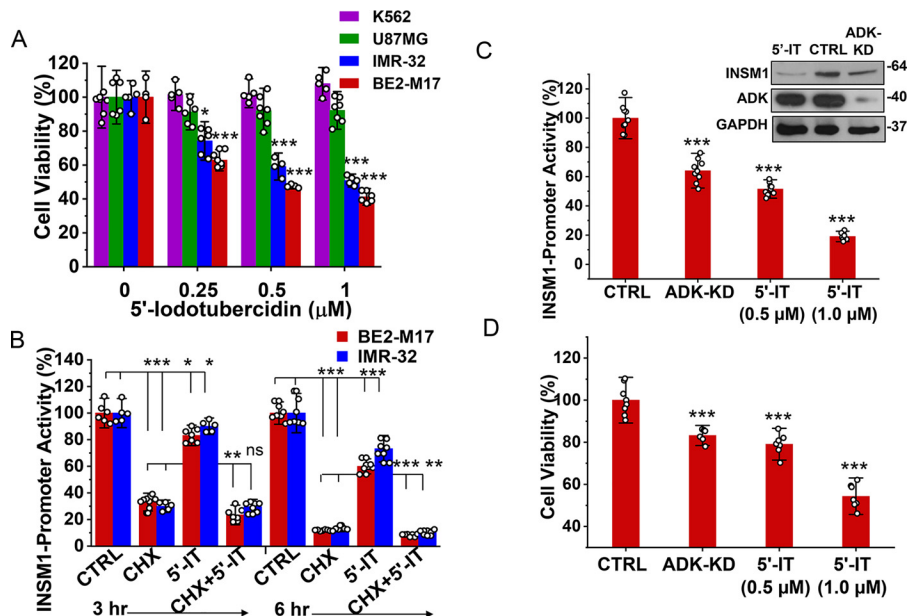
Figure 2. ADK knockdown and cytotoxic effect of 5′-IT in different cell types. *A,* K562 (myelogenous leukemia), U87MG (glioblastoma), IMR-32, and BE2-M17 (NB) cells were treated with different doses of 5′-IT for 72 h. A dose-response MTS assay showed 50% cell viability (0.5 µM) in NB cells, IMR-32 and BE2-M17, but little or no effects in U87MG and K562 cells. Data represent mean ± S.D. ***, $p \leq 0.001$ ($n = 6$–8/group). *B,* INSM1 promoter activity was measured in the presence or absence of cycloheximide in a shorter time point (3 or 6 h) with 5′-IT (1 µM) treatment using BE2-M17 and IMR-32. Data represent mean ± S.D. *, $p \leq 0.05$; **, $p \leq 0.01$; ***, $p \leq 0.001$ ($n = 6$–8/group). *C,* BE2-M17 cells were treated with ADK siRNA for 3 days to KD ADK. INSM1 promoter activity was measured after ADK siRNA KD or 5′-IT treatment. Protein lysates were subjected to Western blotting analyses using ADK, INSM1, or GAPDH antibody. Data represent mean ± S.D. ***, $p \leq 0.001$ ($n = 6$–8/group). *D,* ADK KD MTS assay was performed in a 96-well setting for 72 h. Data represent mean ± S.D. ***, $p \leq 0.001$ ($n = 6$–8/group).

INSM1-promoter activity showed incremental suppression (0.25–1.0 µM) in BE2-M17 and IMR-32 cells (Fig. 1*B*). 5′-IT treatment of BE2-M17 and/or IMR-32 cells down-regulated INSM1 expression in a real-time PCR and Western blotting analyses (Fig. 1, *C* and *D*). Inversely, overexpression of INSM1 or N-Myc in BE2-M17 cells partially restores cell viability from 5′-IT–induced cell death (Fig. 1*E*). This result strongly suggests that INSM1 and/or N-Myc expression is critically important for NB cell survival, which responds to 5′-IT treatment. Both IMR-32 and BE2-M17 showed 50% cell viability at 0.5 µM, but little or no effect was observed in glioblastoma (U87MG), or myelogenous leukemia (K562) cells (Fig. 2*A*). However, 5′-IT inhibits ADK and perturbs adenosine balance in cell metabolism that poses varying degrees of tumor cell cytotoxicity including NB. We performed the reporter assay in the presence or absence of cycloheximide in a shorter time point (3 or 6 h) with 5′-IT (1 µM) treatment (Fig. 2*B*). Cycloheximide (10 µg/ml) alone suppresses INSM1 promoter activity greatly, whereas 5′-IT suppresses INSM1 promoter activity significantly in 3 or 6 h. Suppression of INSM1 promoter activity by cycloheximide suggests that INSM1 promoter activity is depended upon *de novo* protein synthesis. Comparison of the cycloheximide alone and cycloheximide + 5′-IT showed significant enhanced inhibition in BE2-M17 but not IMR-32 cells in 3 h. However, after 6 h treatment, both cell lines showed significant inhibitory enhancement suggesting that 5′-IT acts on INSM1 promoter activity more than *de novo* protein synthesis. The effect of 5′-IT on the INSM1 expression (3 h) precedes the growth inhibition (>24 h).

Knockdown of ADK exhibits similar effects as 5′-IT in NB

To validate the specific inhibition of ADK by 5′-IT results from INSM1 down-regulation leading to NB cell cytotoxicity, BE2-M17 cells were subjected to ADK siRNA knockdown (KD) for 72 h. ADK-KD suppressed ADK expression and the INSM1-promoter activity similar to 5′-IT treatment. However, 5′-IT only blocked the ADK signaling pathway, but did not down-regulate ADK protein levels directly (Fig. 2*C*, *upper right*). Furthermore, the 3-(4,5-dimethyl-2-yl)-5-(3-carboxymethoxyphenyl)-2-(4-sulfophenyl)-2*H*-tetrazolium (MTS) assay revealed that knockdown of ADK expression also decreased cellular viability consistent with 5′-IT inhibition of the ADK signaling pathway (Fig. 2*D*).

5′-IT blockage of the ADK pathway increases intracellular adenosine and the consumption of extracellular adenosine through adenosine receptor-3 signaling pathway

How the ADK inhibitor (ADKi, 5′-IT) affects NB tumor cell growth was further investigated. The first step of this study is to dissect the functional effects of adenosine imbalance using specific inhibitors to block alternative signaling pathways controlling intra- and extracellular adenosine levels to establish how they contribute to the down-regulation of INSM1 leading to reduced NB tumor cell growth. Other studies have revealed that activation of the AMPK inhibits the proliferation of human endothelial cells (15). In the NB system, 5′-IT exhibits an inhibitory effect in contrast to facilitating NB tumor cell growth. Therefore, the 5′-IT blockage of the ADK pathway (AMPK) does not contribute to the negative effect on NB tumor cell growth. Other mechanisms that control NB cell viability via
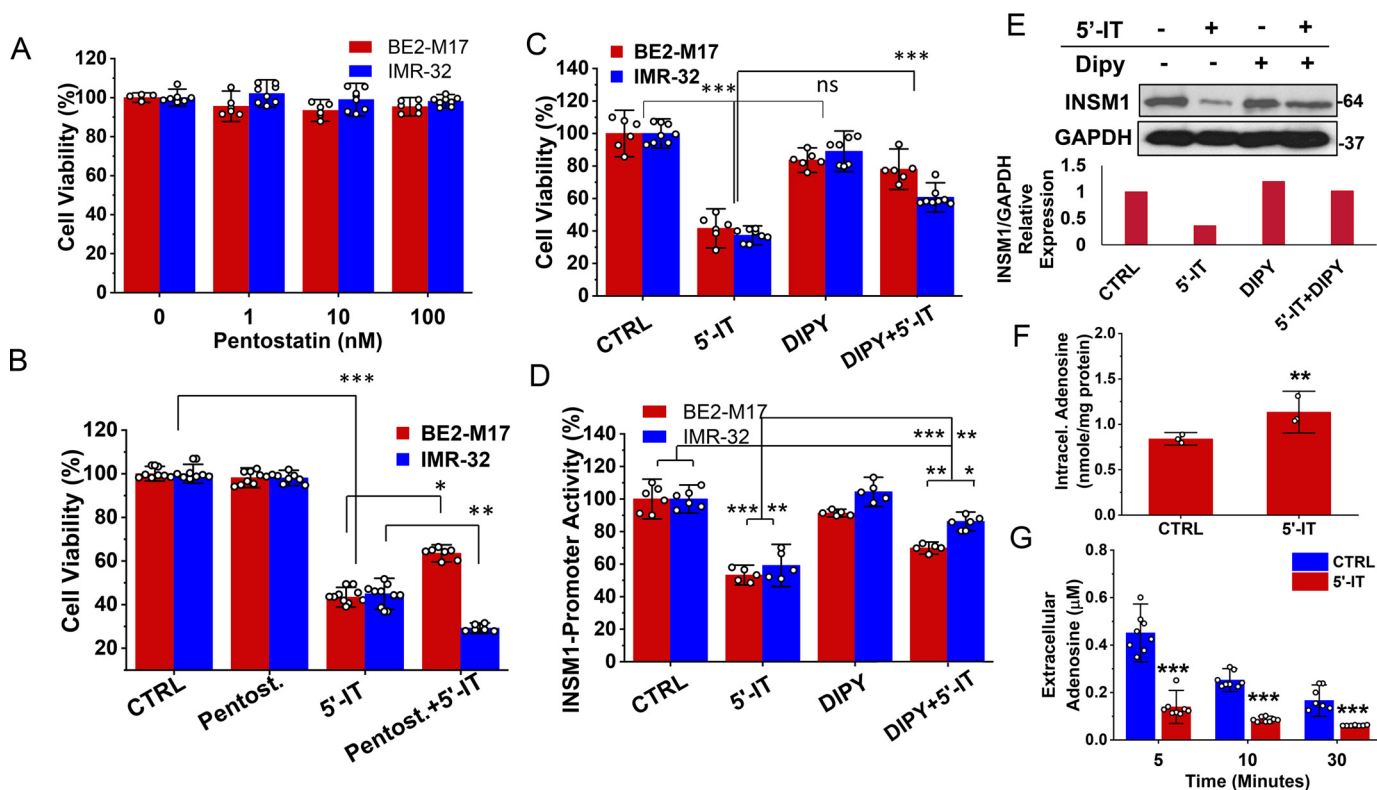
Figure 3. 5′-IT, pentostatin, and/or dipyridamole effects in NB. *A,* pentostatin (0–100 nᴍ)-treated NB cell viability. *B,* combination of pentostatin (100 nᴍ) with or without 5′-IT (1 μᴍ) exerts opposite effects in BE2-M17 and IMR-32 cells. It reduces the BE2-M17 cytotoxic effect, but enhances the IMR-32 cytotoxic effect. Data represent mean ± S.D. *, $p \leq 0.05$; **, $p \leq 0.01$; ***, $p \leq 0.001$ ($n = 6–8$/group). *C,* nucleoside transporter inhibitor (dipyridamole, 10 μᴍ) has little effect on NB cell viability, but a combination of 5′-IT (1 μᴍ) with dipyridamole (10 μᴍ) showed a moderate lessening effect on 5′-IT cytotoxicity. Data represent mean ± S.D. ***, $p \leq 0.001$ ($n = 6–8$/group). *D,* BE2-M17 cells were treated with DMSO, 5′-IT (0.5 μᴍ), and/or dipyridamole (10 μᴍ) for 12 h. The dipyridamole restores the 5′-IT effect on INSM1-promoter activity. Data represent mean ± S.D. *, $p \leq 0.05$; **, $p \leq 0.01$; ***, $p \leq 0.001$ ($n = 6–8$/group). *E,* INSM1 protein expression was partially restored by dipyridamole (10 μᴍ) treatment. *F,* BE2-M17 cells treated with 5′-IT (1.0 μᴍ) for 24 h increased intracellular adenosine concentration (nmol/mg of protein). Data represent mean ± S.D. **, $p \leq 0.01$ ($n = 3$/group). *G,* medium collected from control or 5′-IT–treated BE2-M17 cells (1 × 10⁷) at various time points (5–30 min) was subjected to RP-HPLC analysis. Extracellular adenosine from 5′-IT–treated (1 μᴍ) *versus* control medium are shown in micromolar concentration. Data represent mean ± S.D. ***, $p \leq 0.001$ ($n = 6–8$/group).

5′-IT treatment could include increases of intracellular adenosine levels direct toward the formation of intracellular inosine through adenosine deaminase (ADA) or by directing a re-balance of the intra- and extracellular adenosine levels through the nucleoside transporter (NT). BE2-M17 or IMR-32 cells were treated with the ADA inhibitor (pentostatin) alone (Fig. 3*A*). ADA inhibitor alone has little cytotoxic effects to the cells. However, a combination of the ADA inhibitor with 5′-IT shows an opposite effect on BE2-M17 *versus* IMR-32 cells. Pentostatin slightly restores BE2-M17 cell viability in contrast to the slight decreases in IMR-32 cell viability suggesting that perturbation of intracellular adenosine levels through the ADA pathway could either reduce or enhance 5′-IT cytotoxicity (Fig. 3*B*). The NT inhibitor (dipyridamole) alone has no significant effects on cell viability. When an NT inhibitor (dipyridamole) and 5′-IT were used, the result shows a moderate lessening of 5′-IT cytotoxicity and increase in INSM1 promoter activity in both cell lines (Fig. 3, *C* and *D*). Addition of NT inhibitor in 5′-IT–treated cells also restores the down-regulated INSM1 protein expression partially in BE2-M17 cells (Fig. 3*E*). These results suggest that blockage of NT could reduce adenosine export and 5′-IT cytotoxicity. Using reverse phase HPLC analysis, intracellular adenosine concentration (nmol/mg protein) increased upon 5′-IT treatment for 24 h (Fig. 3*F*). Additionally, 5′-IT

treatment blocks the extracellular ADK signaling pathway, which facilitates extracellular adenosine interaction with the adenosine receptor-3 (ARA₃) pathway. The control medium adenosine concentration at the 5-min time point reached ∼4.5 μᴍ, which is higher than the ARA₃ activated concentration (EC₅₀: 0.29 μᴍ) (16). Clearly, 5′-IT treatment facilitates the usage of extracellular adenosine to activate ARA₃ faster than the control group in a time period between 5 and 30 min (Fig. 3*G*).

Altered adenosine balance triggers adenosine receptor-3 (ARA₃) signaling pathway

An interesting observation reveals that human NB tumor cells (BE2-M17 and IMR-32) do not express ARA₂ₐ, but express a moderate level of ARA₁ and ARA₃, and high level of ARA₂ᵦ adenosine receptors. ARA₁ is coupled to pertussis toxin-sensitive Gᵢ proteins that lead to inhibition of adenylyl cyclase activity (17). ARA₂ᵦ is known to be a low-affinity AR playing a major role in inflammation (18), whereas ARA₃ is the only adenosine subtype to be overexpressed in inflammatory and cancer cells (19). Because ARA₁, ARA₃, or ARA₂ᵦ exhibit opposite effects of either inhibiting or activating adenylate cyclase, they are destined to modulate the cAMP signaling pathway. An agonist for ARA₁ (N^6-cyclopentyladenosine (CPA)), ARA₃ (2-Cl-IB-MECA), or ARA₂ᵦ (BAY606583) was tested with or without

SASBMB

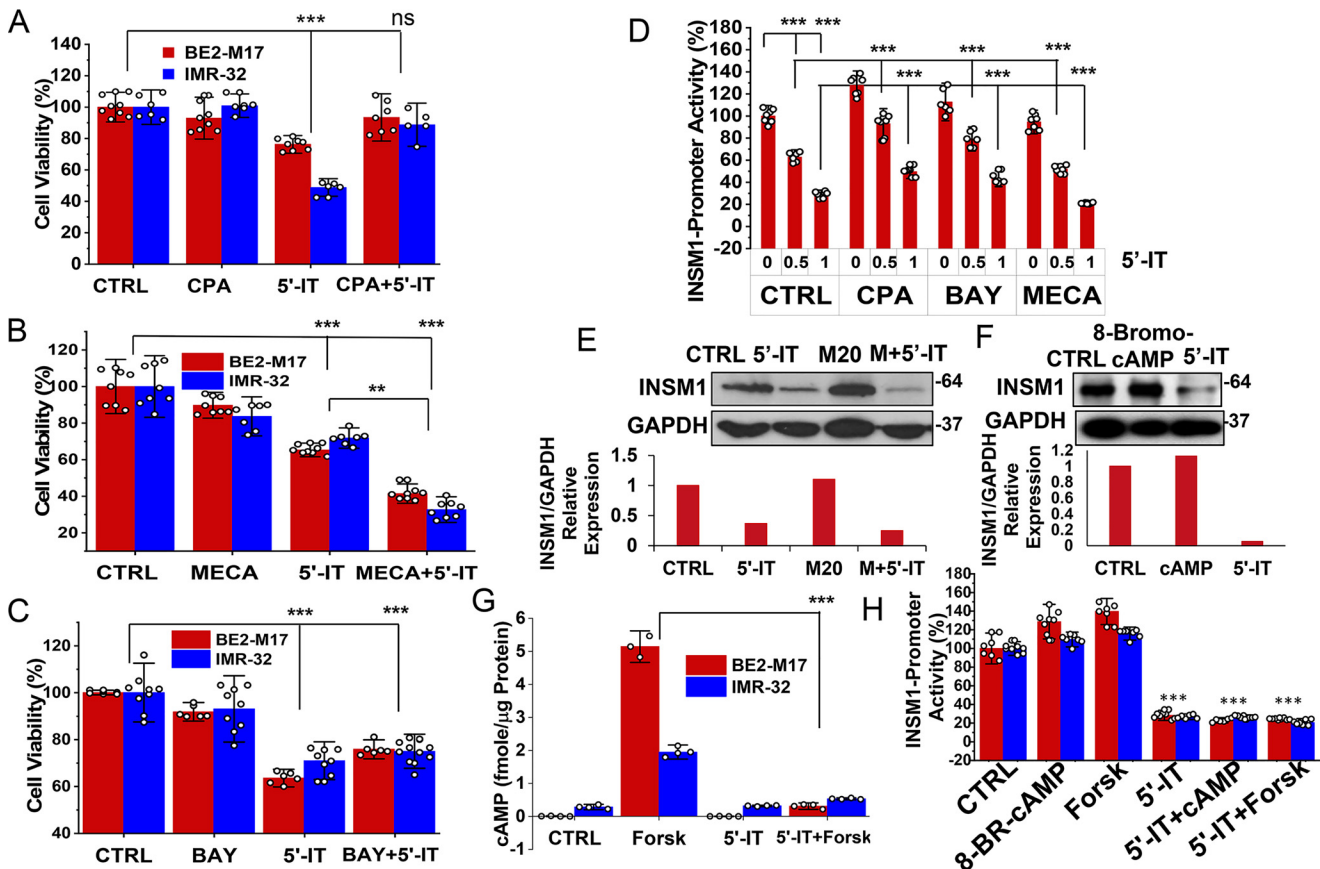*J. Biol. Chem.* (2019) 294(14) 5456–5465 **5459**

Figure 4. 5′-IT triggers adenosine receptor-3–mediated cAMP response. *A,* single or a combination of 5′-IT (0.5 μM) and CPA (100 μM) treatments for 3 days in MTS assay. Data represent mean ± S.D. ***, $p \leq 0.001$ ($n = 6-8$/group). *B,* single or a combination of 5′-IT (0.5 μM) and 2-Cl-IB-MECA (20 μM) treatments for 3 days in MTS assay. Data represent mean ± S.D. **, $p \leq 0.01$; ***, $p \leq 0.001$ ($n = 6-9$/group). *C,* single or a combination of 5′-IT (0.5 μM) and BAY606583 (20 μM) treatments for 3 days in MTS assay. Data represent mean ± S.D. ***, $p \leq 0.001$ ($n = 6-9$/group). *D,* INSM1 promoter-directed luciferase activity was measured after BE2-M17 cells were treated with 5′-IT and/or CPA (100 μM), 2-Cl-IB-MECA (20 μM), and BAY606583 (20 μM) for 6 h. A shorter time treatment protocol is designed to reveal the 5′-IT effect on the INSM1 promoter voiding the cytotoxic effect of 5′-IT. Data represent mean ± S.D. ***, $p \leq 0.001$ ($n = 6-8$/group). *E* and *F,* 8-bromo-cAMP (20 μM), 5′-IT (1 μM), and/or 2-Cl-IB-MECA (20 μM) treatments of BE2-M17 cells affects INSM1 expression. *G,* BE2-M17 and IMR-32 cells were treated with phosphodiesterase inhibitor, Ro-20-1724 (100 μM) and forskolin (10 μM) first and subsequently 5′-IT (1 μM) was added for an additional 30 min. Cellular cAMP levels were measured using cAMP ELISA kit. cAMP levels are present as fmol/μg of protein. Data represent mean ± S.D. ***, $p \leq 0.001$ ($n = 4$/group). *H,* INSM1 promoter activity was measured in 5′-IT, 8-bromo-cAMP, forskolin, 5′-IT and 8-bromo-cAMP, or 5′-IT and forskolin–treated NB cells. Data represent mean ± S.D. ***, $p \leq 0.001$ ($n = 6-8$/group).

5′-IT in NB tumor cells. In combination with low dose 5′-IT (0.5 μM) and CPA (100 μM), 2-Cl-IB-MECA (20 μM) or BAY606583 (20 μM), only 2-Cl-IB-MECA exhibits an additive killing effect (Fig. 4B). In contrast, CPA or BAY606583 lessens 5′-IT cytotoxicity (Fig. 4, *A* and *C*). This result suggests that 5′-IT induces an intra- and extracellular adenosine imbalance that facilitates further interaction with ARA₃. INSM1 promoter activity is inhibited by 5′-IT alone or showed and enhanced inhibitory effect in the presence of ARA₃ agonist (2-Cl-IB-MECA). Alternatively, the ARA₁ agonist (CPA), or ARA₂ᵦ agonist (BAY606583) lessens the inhibitory effect with 5′-IT on the NB cells suggesting that ARA₃ signaling mediated the post-5′-IT effects (Fig. 4D). Similarly, INSM1 protein inhibition is consistent with 5′-IT or 5′-IT + 2-Cl-IB-MECA treatment (Fig. 4E). In contrast to 5′-IT treatment, exogenously added 8-bromo-cAMP does not change INSM1 protein expression (Fig. 4F).

5′-IT triggers ARA₃ signaling pathway for the suppression of cAMP

Stimulation of the ARA₃ signaling pathway mediates suppression of adenylyl cyclase and cAMP levels. BE2-M17 or

IMR-32 cells were treated with forskolin (as a stimulator of adenylyl cyclase) for 30 min, followed by treatment with 5′-IT (1.0 μM) in the presence of 100 μM Ro-20-1724 (a phosphodiesterase inhibitor) for an additional 30 min. Following treatment, cAMP content of the acid cell extracts was measured using a cAMP ELISA kit normalized with total cellular protein concentration. Because endogenous cAMP before or after 5′-IT treatment was too low to be reliably detected, forskolin was used to increase the baseline levels of cAMP in the cells. Therefore, cells were pretreated with forskolin before the addition of 5′-IT. Forskolin stimulation of cAMP was completely suppressed by 5′-IT treatment (Fig. 4G). 5′-IT down-regulates cAMP and INSM1 promoter activity. We measured INSM1 promoter activity using BE2-M17 and IMR-32 cells by adding forskolin, 8-bromo-cAMP (exogenous cAMP), 5′-IT, 5′-IT + forskolin, or 5′-IT + 8-bromo-cAMP. Forskolin or 8-bromo-cAMP slightly increases INSM1 promoter activity, whereas 5′-IT alone, 5′-IT and forskolin, or 5′-IT and 8-bromo-cAMP overrides INSM1 promoter activity. Addition of forskolin or 8-bromo-cAMP does not inhibit the INSM1 expression (Fig. 4, *F* and *H*).
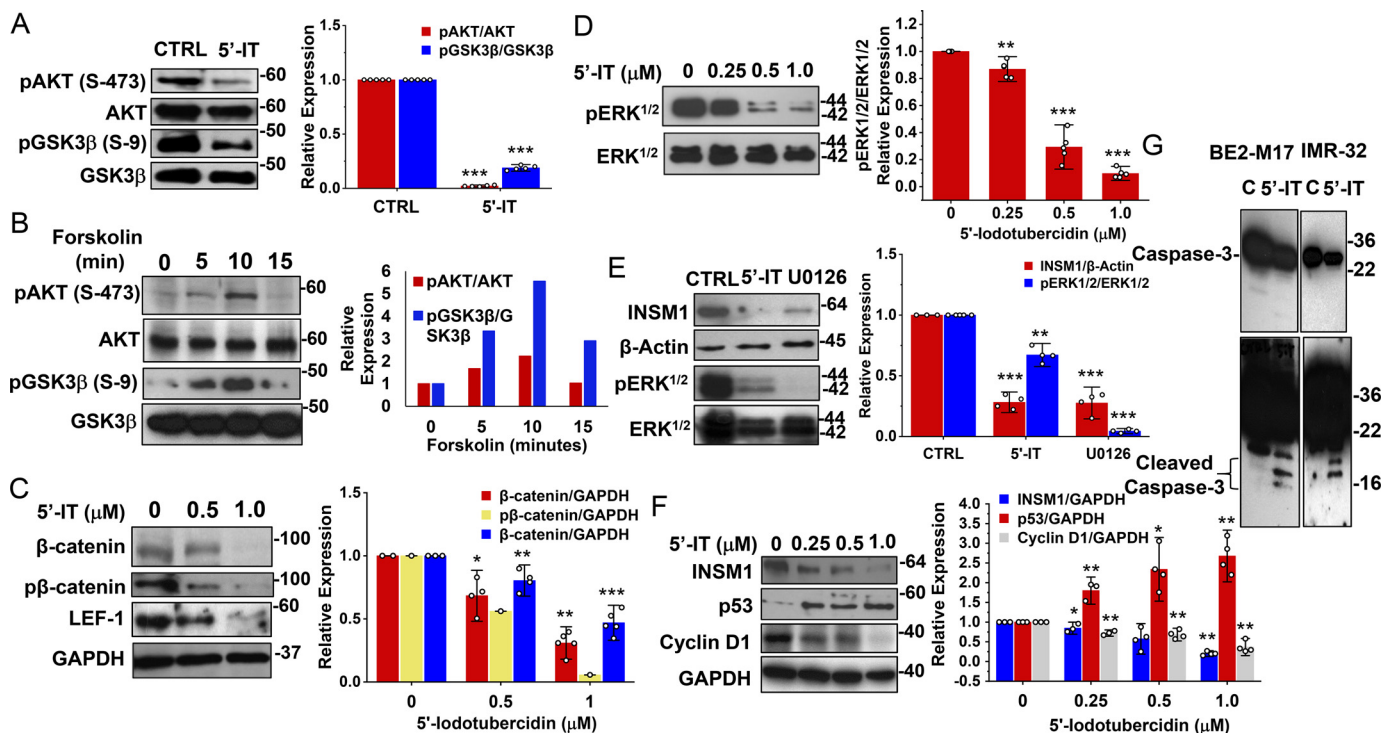
Figure 5. 5'-IT effects in BE2-M17 cells. *A,* BE2-M17 cells were treated with control (DMSO) or 5'-IT (1 μM) for 3 days before being subjected to Western blot analysis using the indicated antibodies. Data represent mean ± S.D. ***, $p \leq 0.001$ ($n = 5$/group). *B,* BE2-M17 cells were starved overnight, treated with forskolin (10 μM) for various time points (0–15 min). Phospho-AKT (S-473) and pGSK3β were detected *versus* pan-AKT and GSK3β antibody. *C–F,* BE2-M17 cells were treated with the indicated dose of 5'-IT (1 μM) or U0126 (10 μM) for 3 days before being subjected to Western blot analysis using the indicated antibody. Data represent mean ± S.D. *, $p \leq 0.05$; **, $p \leq 0.01$; ***, $p \leq 0.001$ ($n = 3–5$/group). *G,* BE2-M17 and IMR-32 cells were treated with DMSO (control) or 5'-IT (1 μM) and Western blot analysis for caspase-3. *Upper panel* shows a very short film exposure (2 s) of caspase-3 *versus* a longer film exposure (*lower panel*), which exhibits 5'-IT induction of cleaved caspase-3.

5'-IT modulates cAMP via ARA$_3$ signaling leading to cell growth inhibition

5'-IT–treated BE2-M17 cells trigger ARA$_3$ signaling leading to suppression of cAMP. Suppression of cAMP decreased AKT and GSK3β phosphorylation thus resulting in increased GSK3β activity triggering β-catenin phosphorylation and degradation (Fig. 5, *A and C*). Inversely, exogenously added forskolin activated adenylyl cyclase that stimulates cAMP, AKT, and GSK3β phosphorylation that peaked at 10 min (Fig. 5B). β-Catenin phosphorylation and LEF-1 expression were down-regulated upon 5'-IT treatment (Fig. 5C). Additionally, 5'-IT also down-regulated ERK1/2 phosphorylation that is critical for cell proliferation and cross-talk with the AKT pathway (Fig. 5D). Blockage of the ERK1/2 pathway (U0126) inhibits INSM1 protein expression similar to the effect of 5'-IT supporting cross-talk between the AKT and ERK1/2 signaling pathways (Fig. 5E). 5'-IT induces apoptosis via down-regulation of INSM1 and cyclin D1 in addition to the observed activation of both p53 and caspase-3 (Fig. 5, *F and G*). These results suggest that the inhibition of ADK and ERK1/2 pathways resulted in INSM1 suppression, which plays a critical role in the inhibition of NB cell proliferation and induction of programmed cell death.

Discussion

Due to the importance of the transcriptional regulator INSM1 on the proliferation of NB cells, an INSM1 promoter-driven luciferase screening platform was used to target associated signaling pathways that lead to the down-regulation of INSM1 expression in NB. A novel ADKi, 5'-IT, was identified that exhibited potent inhibition of INSM1 expression and NB tumor cell growth. The molecular mechanisms underlying how 5'-IT suppressed the ADK pathway that contributes to the inhibition of NB cell growth was further investigated. Three different pathways associated with adenosine perturbation via ADK inhibition were tested. These pathways include the balance of adenosine and AMPK toward the energy-sensing pathway, increase of intracellular adenosine that triggers inosine formation via ADA, or a re-balance of the intra- and extracellular adenosine levels through the NT (Fig. 6). Adenosine was shown to induce apoptosis in human gastric cancer cells via activation of the AMP-activated protein kinase (20). Similarly, activation of the AMP-activated protein kinase inhibits the proliferation of human endothelial cells (15). In contrast, blockage of the AMP-activated protein kinase pathway by 5'-IT promotes beta-cell proliferation and cell growth (21), which is opposite from our observation that 5'-IT suppresses NB tumor cell growth. Therefore, it is unlikely that blockage of the AMPK signaling pathway contributes to NB cell death. Using the ADA inhibitor (pentostatin) that targets the inosine synthesis pathway reveals that 5'-IT alters adenosine concentration and could only slightly reduce or enhance the 5'-IT cytotoxicity in the NB cells. Whereas the NT inhibitor (dipyridamole) blocks adenosine export and consistently lessened the 5'-IT cytotoxicity to the NB cells. An interesting observation in our work reveals that 5'-IT re-balances intracellular adenosine and directs extracellular adenosine to trigger the ARA$_3$ signaling pathway. The
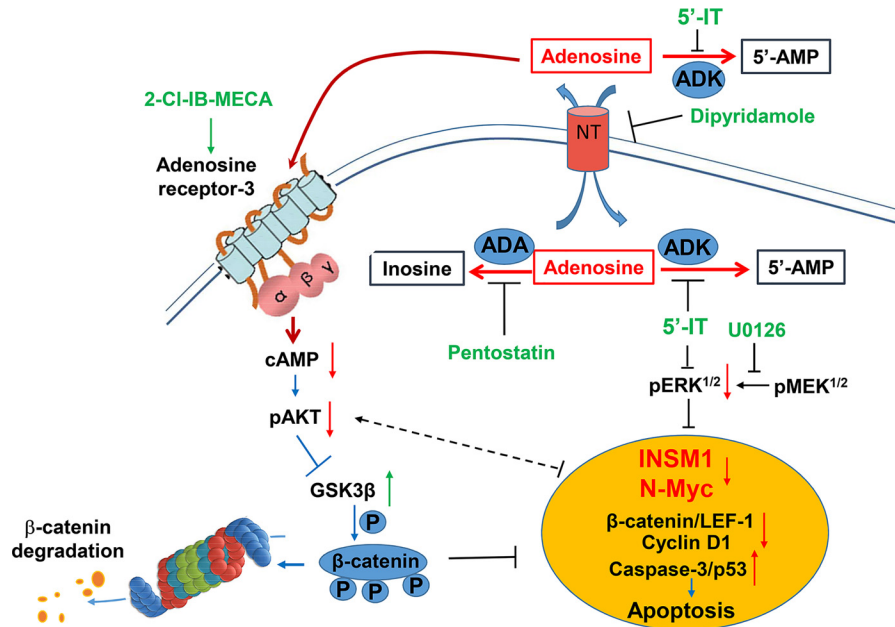
Figure 6. 5′-IT treatment affects intra-/extracellular adenosine balance and INSM1 expression leading to NB tumor cell death. 5′-IT controls intra-/extracellular adenosine that mediates through the inhibition of ADK via the AMP signaling pathway. Intracellular adenosine could also direct the inosine pathway through ADA (ADA inhibitor, pentostatin). Imbalance of intra-/extracellular adenosine promotes adenosine export through the nucleoside transporter (NT, NT inhibitor, dipyridamole). Extracellular adenosine triggers the adenosine receptor-3 (ARA₃) signaling pathway resulting in the suppression of cAMP, which enhances β-catenin phosphorylation toward cytoplasmic proteasomal degradation. 5′-IT, pentostatin, U0126, and dipyridamole (*green labels*) are inhibitors for ADK, ADA, MEK1/2-ERK1/2, and NT pathways. 2-Cl-IB-MECA is an ARA₃ agonist. 5′-IT down-regulates pAKT, pGSK3β, β-catenin, LEF-1, pERK1/2, cyclin D1, INSM1, N-Myc and activates caspase-3, and p53 for NB apoptosis.

observation was confirmed by HPLC analyses of intra- and extracellular adenosine concentration as well as using 5′-IT and ARA₃ agonist for combined treatment of NB cells. Our data suggests that agonist activation of the ARA₃ signaling pathway potentiates the observed ADKi effect and INSM1 inhibition leading to reduced cell viability of NB cells.

Adenosine is considered a major regulator of local tissue function. There are four types of adenosine receptors including ARA₁, ARA₂ₐ, ARA₂ᵦ, and ARA₃. Our study showed that inhibition of the ADK signaling pathway perturbs the balance of intra- and extracellular adenosine levels via the ARA₃ in NB cells. This hypothesis is further substantiated by use of the ARA₃ agonist (2-Cl-IB-MECA) that causes the down-regulation of cAMP via the ARA₃ signaling pathway. Suppression of cAMP decreases AKT (Ser-473) phosphorylation and activates GSK3β activity. GSK3β induces β-catenin phosphorylation, which thereby targets phosphorylated β-catenin for proteasomal degradation and subsequent NB cell apoptosis. Furthermore, we present evidence that 5′-IT inhibits the ERK1/2 signaling pathway, which is consistent with ARA₃ activation that inhibits cell proliferation via the PI3K/AKT-dependent inhibition of the ERK1/2 phosphorylation in A375 human melanoma cells (22). In parallel, INSM1 expression is positively correlated with AKT and ERK1/2 phosphorylation (12, 23). Both down-regulation of AKT and ERK1/2 phosphorylation by 5′-IT could be due to the inhibition of INSM1 expression as well as triggering the ARA₃ signaling pathway. Therefore, targeting ADK and the ARA₃ pathway could lead to the inhibition of NB cell growth and the promotion of apoptosis. These findings are significant because they could develop a novel pre-clinical treatment for aggressive forms of human NB (Fig. 6).

The current study established an INSM1 promoter-driven luciferase reporter assay to identify positive hits on regulation of INSM1 promoter activity, which in parallel correlates with NB tumor cell growth. Our most significant hit supports that the ADK signaling pathway inhibitor 5′-IT modulates INSM1 and N-Myc expression and targets NB cell growth through intra- and extracellular adenosine re-balance, which triggers the ARA₃ signaling pathway. Specifically, the ARA₃ agonist demonstrates anti-inflammatory and anti-cancer effects via a molecular mechanism that entails modulation of the Wnt and the NF-κB signal transduction pathways (24, 25). ARA₃ agonists were developed for the treatment of anti-tumor, inflammatory, ophthalmic, and liver diseases and demonstrate excellent safety and efficacy in phase 2 clinical studies (26–28). The outcome of this study enhances our understanding of the underlying mechanisms that leads to NB tumor cell growth and provides us with new insights for the novel combinational treatment options against this aggressive tumor.

In summary, INSM1 is a specific NE tumor marker critical for aggressive NB tumor cell growth and invasion. Knockdown of INSM1 suppresses NB tumor growth *in vivo* (12). We used an INSM1 promoter-driven luciferase reporter assay to identify drugs that specifically inhibit INSM1 promoter activity. 5′-IT was identified to suppress INSM1 promoter and NB tumor cell growth. However, 5′-IT was originally considered as a general kinase inhibitor, especially ADK due to its affinity for the ATP-binding sites of these enzymes and has been shown to affect cell proliferation and survival. 5′-IT could cause DNA damage and activate the Atm-p53 pathway as a genotoxic drug with anti-colon cancer potential (29). 5′-IT suppresses INSM1 promoter activity led us to investigate additional pathways associated

with INSM1 expression in aggressive NB. The outcomes of this study revealed that 5′-IT not only suppresses INSM1 expression, but also triggers ARA$_3$ signaling and AKT/ERK1/2 phosphorylation pathways, which could contribute to the inhibition of NB cell proliferation and the promotion of apoptosis.

Experimental procedures

Cell culture and reagents

Human NB cell lines, IMR-32 and BE2-M17, glioblastoma cell line, U87MG, and chronic myelogenous leukemia cell line, K562, were obtained from the American Type Culture Collection (Manassas, VA). Cells were cultured in RPMI 1640 medium supplemented with 10% fetal bovine serum (Atlanta Biological Inc., Flowery Branch, GA), 1× penicillin/streptomycin in 5% CO$_2$ incubator at 37 °C. All the cell lines were authenticated with Short Tandem Repeat DNA profiling analysis. The passage number of the cells used for the experiments was kept under 35. 5′-IT, pentostatin, dipyridamole, 8-bromo-cAMP, CPA, RA, DAPT, 5′-aza-2 deoxycytidine, and forskolin were purchased from Sigma. GANT58, GANT61, 2-Cl-IB-MECA, and BAY606583 were purchased from Tocris Bioscience (Minneapolis, MN). LY294002, U0126, and TCA were purchased from Cell Signaling Technologies (Danvers, MA). ZM336372 was purchased from Enzo Life Science (Farmingdale, NY). Ro-20-1724 was purchased from EMD Millipore Corporation (Burlington, MA). Antibodies, INSM1 (A8, sc-271408), N-Myc (B8.4B, sc-53993), ADK (F-5, sc-365470), and LEF-1 were purchased from Santa Cruz Biotechnology (Dallas, TX). pAKT (Ser-473, 4060), AKT (2920), pGSK3β (Ser-9), GSK3β, pMAPK42/44 (Thr-202/Tyr-204, 9101), MAPK42/44 (9102), β-catenin, p53, caspase-3 (9662), and cyclin D1 were purchased from Cell Signaling Technology. Antibody to GAPDH was purchased from Life Technologies and actin antibody was obtained from Sigma. Horseradish peroxidase-conjugated secondary antibody was obtained from Bio-Rad Laboratories. ADK siRNA (sc-38902) was purchased from Santa Cruz Biotechnology and transfected with Lipofectamine RNAiMAX transfection protocol (Life Technologies).

Real-time RT-PCR

RNA were extracted with TRIzol reagent and treated with 2 units of DNase I (Promega, Madison, WI) to digest genomic DNA. cDNA synthesis using the High Capacity RNA-to-cDNA^{TM} Kit (Life Tech.) followed the manufacturer's protocol. RNA was reverse-transcribed and analyzed by real-time PCR for the expression of INSM1, N-myc, and GAPDH. The relative RNA concentration of the target gene was normalized with GAPDH. Primers for INSM1: forward, 5′-ACGGAATTCTGCCACCTGTGCCC-AGTGTGCGGAGAG-3′, reverse, 5′-CACCTCGAGCTAGCA-GGCCGGGCGCACGGGCACCTGCAG-3′; and primers for N-Myc: forward, 5′-CCCTGAGCGATTCAGATGA-3′, reverse, 5′-GACGCACAGTGATGGTGAAT-3′, were used. The INSM1, N-Myc primers and probes for real-time PCR were purchased from Life Technologies.

MTS assay

MTS proliferation assay was carried out according to the manufacturer's protocol. In brief, each group of cells were treated with the indicated concentrations of compounds for 72 h. Treated cells were collected and incubated in medium containing 20 μl of MTS assay reagent (Abcam, Cambridge, MA) at 37 °C for 4 h. The assay was read at absorbance (490 nm) using a 96-well plate spectrophotometer to calculate cell viability.

INSM1 promoter-driven luciferase reporter assay

An INSM1 promoter ($-426/+40$ bp) was inserted into pGL4.18-[luc2P/Neo] basic vector (Promega Co.) in front of a *luciferase 2* (*Luc2*) gene. INSM1 reporter plasmid was linearized and transfected into BE2-M17 or IMR-32 NB cells with Lipofectamine 2000 (Invitrogen) for 48 h. Transfected cells were selected with a pre-determined G418 concentration in culture medium for 2 weeks. The G418-selected stable cells were further assayed for the INSM1 promoter-driven *Luc2* activity. The strong luciferase activity reflects strong INSM1 promoter activity in each cell line. For the INSM1 promoter screening assay, cells were seeded in a 96-well plate overnight, then treated with each indicated test compound for 24 to 72 h. After treatment, the luciferase activity was analyzed with Firefly Luciferase Assay Kit 2.0 (Biotium Inc., Fremont, CA).

Western blot analysis

Cell lysates were extracted with lysis buffer (10 mM Tris-HCl, pH 7.5, 150 mM NaCl, 10% glycerol, 1% Triton X-100, 1 mM DTT, 0.2 mM PMSF, 1 μg/ml of aprotinin, 1 μg/ml of leupeptin, 1 mM Na$_3$VO$_4$, and 5 mM NaF) and separated by SDS-PAGE. The electrophoresed proteins were electrotransferred onto a nitrocellulose membrane (Bio-Rad) for Western blotting analyses. The membrane was blocked with 5% nonfat dry milk in TBST (20 mM Tris-HCl, pH 7.6, 137 mM NaCl, and 0.1% Tween 20), probed with the indicated primary antibody overnight at 4 °C, and bound with horseradish peroxidase-conjugated secondary antibody at room temperature for 1 h. The blot was developed with chemiluminescence substrate (Bio-Rad) and exposed on X-ray film (Fuji Photo Film Co., Japan). The same blot was striped several times for subsequent antibody blotting. Western blot analysis was repeated a minimum of three separate experiments to ensure reproducibility.

Analysis of adenosine by RP-HPLC

BE2-M17 cells (1×10^7) were treated with 5′-IT (1 μM) for 10–30-min intervals or the indicated time point. Culture medium or cell pellet was isolated and extracted with 0.4 M perchloric acid on ice for 5 min. The solution was centrifuged at 13,000 rpm for 2 min at 4 °C and neutralized with ice-cold 2 M K$_2$CO$_3$ to pH 7.5. Adenosine unknowns were run on a Thermo Scientific Dionex U3000 Ultimate system equipped with a quaternary pump, an autosampler, and a diode array detector, all controlled by Thermo Fisher Dionex Chromeleon 6.8 software. Run conditions were previously established with the following changes ([30]). The run consisted of an isocratic separation in 7% acetonitrile at 0.2 ml/min on a Dionex Acclaim 120 Bonded Silica C18 (5 μm, 120 Å × 2.1 × 150 mm) column with a corresponding 5-mm guard column. Adenosine was monitored at 260 nm, bandwidth 20 nm, using a 20-min run time. A total of 16 adenosine standards were freshly prepared in 7% acetonitrile

by serial dilution between 1000 and 0.01 μM. Standard curves were generated by linear regression analysis and accepted with a $R^2 > 0.999$. Unknowns were run 4 times each and standard deviation was calculated for each. Drift was monitored by repeating standards as unknowns throughout the run.

cAMP assay

BE2-M17 or IMR-32 cells were seeded in 24-well plate overnight. Cells were washed in 500 μl of Hank's balanced salt solution for 10 min at room temperature. Cells were pre-treated with phosphodiesterase inhibitor Ro-20-1724 (100 μM) for 30 min to inhibit endogenous phosphodiesterase activity. Forskolin (10 μM) was added for 15 min before addition of 5′-IT (1 μM) and incubated for an additional 30 min at 37 °C. Cellular cAMP was extracted and measured using a cAMP ELISA kit (Cell Biolabs, Inc., San Diego, CA) according to the manufacturer's instructions.

Statistical analysis

The presented values were calculated and expressed relative to an untreated control group. All experiments were repeated at least three times. Results are presented as mean ± S.D. Statistical analysis was performed using either the Student's t test when only two groups were in the experiment or by one-way analysis of variance comparison of multiple groups using the Tukey-Kramer test with differences at p values of less than 0.05 being considered significant.

References

1. Brodeur, G. M. (2003) Neuroblastoma: biological insights into a clinical enigma. *Nat. Rev. Cancer* **3,** 203–216 CrossRef Medline
2. Maris, J. M., Hogarty, M. D., Bagatell, R., and Cohn, S. L. (2007) Neuroblastoma. *Lancet* **369,** 2106–2120 CrossRef Medline
3. Wildner, H., Gierl, M. S., Strehle, M., Pla, P., and Birchmeier, C. (2008) Insm1 (IA-1) is a crucial component of the transcriptional network that controls differentiation of the sympatho-adrenal lineage. *Development* **135,** 473–481 CrossRef Medline
4. Farkas, L. M., Haffner, C., Giger, T., Khaitovich, P., Nowick, K., Birchmeier, C., Pääbo, S., and Huttner, W. B. (2008) Insulinoma-associated 1 has a panneurogenic role and promotes the generation and expansion of basal progenitors in the developing mouse neocortex. *Neuron* **60,** 40–55 CrossRef Medline
5. Brodeur, G. M., Seeger, R. C., Schwab, M., Varmus, H. E., and Bishop, J. M. (1984) Amplification of N-myc in untreated human neuroblastomas correlates with advanced disease stage. *Science* **224,** 1121–1124 CrossRef Medline
6. Look, A. T., Hayes, F. A., Shuster, J. J., Douglass, E. C., Castleberry, R. P., Bowman, L. C., Smith, E. I., and Brodeur, G. M. (1991) Clinical relevance of tumor cell ploidy and N-myc gene amplification in childhood neuroblastoma: a pediatric oncology group study. *J. Clin. Oncol.* **9,** 581–591 CrossRef Medline
7. Seeger, R. C., Brodeur, G. M., Sather, H., Dalton, A., Seigel, S. E., Wong, K. Y., and Hammond, D. (1985) Association of multiple copies of the N-myc oncogene with rapid progression of neuroblastomas. *N. Engl. J. Med.* **313,** 1111–1116 CrossRef Medline
8. Kohl, N. E., Gee, C. E., and Alt, F. W. (1984) Activated expression of the N-myc gene in human neuroblastomas and related tumors. *Science* **226,** 1335–1337 CrossRef Medline
9. Nisen, P. D., Waber, P. G., Rich, M. A., Pierce, S., Garvin, J. R., Jr., Gilbert, F., and Lanzkowsky, P. (1988) N-myc oncogene RNA expression in neuroblastoma. *J. Natl. Cancer Inst.* **80,** 1633–1637 CrossRef Medline
10. Schwab, M. (1991) Enhanced expression of the cellular oncogene MYCN and progression of human neuroblastoma. *Adv. Enzyme Regul.* **31,** 329–338 CrossRef Medline
11. Slavc, I., Ellenbogen, R., Jung, W. H., Vawter, G. F., Kretschmar, C., Grier, H., and Korf, B. R. (1990) *myc* gene amplification and expression in primary human neuroblastoma. *Cancer Res.* **50,** 1459–1463 Medline
12. Chen, C., Breslin, M. B., and Lan, M. S. (2015) INSM1 increases N-myc stability and oncogenesis via a positive-feedback loop in neuroblastoma. *Oncotarget* **6,** 36700–36712 Medline
13. Maira, S. M., Stauffer, F., Schnell, C., and García-Echeverría, C. (2009) PI3K inhibitors for cancer treatment: where do we stand? *Biochem. Soc. Trans.* **37,** 265–272 CrossRef Medline
14. Li, Q. Q., Hao, J. J., Zhang, Z., Hsu, I., Liu, Y., Tao, Z., Lewi, K., Metwalli, A. R., and Agarwal, P. K. (2016) Histone deacetylase inhibitor-induced cell death in bladder cancer is associated with chromatin modification and modifying protein expression: a proteomic approach. *Int. J. Oncol.* **48,** 2591–2607 CrossRef Medline
15. Peyton, K. J., Liu, X. M., Yu, Y., Yates, B., and Durante, W. (2012) Activation of AMP-activated protein kinase inhibits the proliferation of human endothelial cells. *J. Pharmacol. Exp. Therap.* **342,** 827–834 CrossRef Medline
16. Fredholm, B. B., Irenius, E., Kull, B., and Schulte, G. (2001) Comparison of the potency of adenosine as an agonist at human adenosine receptors expressed in Chinese hamster ovary cells. *Biochem. Pharmacol.* **61,** 443–448 CrossRef Medline
17. van Calker, D., Müller, M., and Hamprecht, B. (1979) Adenosine regulates via two different types of receptors, the accumulation of cyclic AMP in cultured brain cells. *J. Neurochem.* **33,** 999–1005 CrossRef Medline
18. Feoktistov, I., and Biaggioni, I. (1995) Adenosine A2b receptors evoke interleukin-8 secretion in human mast cells: an enprofylline-sensitive mechanism with implications for asthma. *J. Clin. Invest.* **96,** 1979–1986 CrossRef Medline
19. Fishman, P., Madi, L., Bar-Yehuda, S., Barer, F., Del Valle, L., and Khalili, K. (2002) Evidence for involvement of Wnt signaling pathway in IB-MECA mediated suppression of melanoma cells. *Oncogene* **21,** 4060–4064 CrossRef Medline
20. Saitoh, M., Nagai, K., Nakagawa, K., Yamamura, T., Yamamoto, S., and Nishizaki, T. (2004) Adenosine induces apoptosis in the human gastric cancer cells via an intrinsic pathway relevant to activation of AMP-activated protein kinase. *Biochem. Pharmacol.* **67,** 2005–2011 CrossRef Medline
21. Annes, J. P., Ryu, J. H., Lam, K., Carolan, P. J., Utz, K., Hollister-Lock, J., Arvanites, A. C., Rubin, L. L., Weir, G., and Melton, D. A. (2012) Adenosine kinase inhibition selectively promotes rodent and porcine islet beta-cell replication. *Proc. Natl. Acad. Sci. U.S.A.* **109,** 3915–3920 CrossRef Medline
22. Merighi, S., Benini, A., Mirandola, P., Gessi, S., Varani, K., Leung, E., Maclennan, S., and Borea, P. A. (2005) A3 adenosine receptor activation inhibits cell proliferation via phosphatidylinositol 3-kinase/Akt-dependent inhibition of the extracellular signal-regulated kinase 1/2 phosphorylation in A375 human melanoma cells. *J. Biol. Chem.* **280,** 19516–19526 CrossRef Medline
23. Chen, C., Breslin, M. B., and Lan, M. S. (2018) Sonic hedgehog signaling pathway promotes INSM1 transcription factor in neuroendocrine lung cancer. *Cell Signal.* **46,** 83–91 CrossRef Medline
24. Fishman, P., Bar-Yehuda, S., Ardon, E., Rath-Wolfson, L., Barrer, F., Ochaion, A., and Madi, L. (2003) Targeting the A3 adenosine receptor for cancer therapy: inhibition of prostate carcinoma cell growth by A3AR agonist. *Anticancer Res.* **23,** 2077–2083 Medline

ASBMB

25. Bar-Yehuda, S., Stemmer, S. M., Madi, L., Castel, D., Ochaion, A., Cohen, S., Barer, F., Zabutti, A., Perez-Liz, G., Del Valle, L., and Fishman, P. (2008) The A3 adenosine receptor agonist CF102 induces apoptosis of hepatocellular carcinoma via de-regulation of the Wnt and NF-κB signal transduction pathways. *Int. J. Oncol.* **33,** 287–295 Medline

26. Cohen, S., Stemmer, S. M., Zozulya, G., Ochaion, A., Patoka, R., Barer, F., Bar-Yehuda, S., Rath-Wolfson, L., Jacobson, K. A., and Fishman, P. (2011) CF102 an A3 adenosine receptor agonist mediates anti-tumor and anti-inflammatory effects in the liver. *J. Cell Physiol.* **226,** 2438–2447 CrossRef Medline

27. Fishman, P., Bar-Yehuda, S., Liang, B. T., and Jacobson, K. A. (2012) Pharmacological and therapeutic effects of A3 adenosine receptor agonists. *Drug Discov. Today* **17,** 359–366 CrossRef Medline

28. Stemmer, S. M., Benjaminov, O., Medalia, G., Ciuraru, N. B., Silverman, M. H., Bar-Yehuda, S., Fishman, S., Harpaz, Z., Farbstein, M., Cohen, S., Patoka, R., Singer, B., Kerns, W. D., and Fishman, P. (2013) CF102 for the treatment of hepatocellular carcinoma: a phase I/II, open-label, dose-escalation study. *Oncologist* **18,** 25–26 CrossRef Medline

29. Zhang, X., Jia, D., Liu, H., Zhu, N., Zhang, W., Feng, J., Yin, J., Hao, B., Cui, D., Deng, Y., Xie, D., He, L., and Li, B. (2013) Identification of 5-iodotubercidin as a genotoxic drug with anti-cancer potential. *PLoS ONE* **8,** e62527 CrossRef Medline

30. Marin, R. M., Franchini, K. G., and Rocco, S. A. (2007) Analysis of adenosine by RP-HPLC method and its application to the study of adenosine kinase kinetics. *J. Sep. Sci.* **30,** 2473–2479 CrossRef Medline

⧫ASBMB

J. Biol. Chem. (2019) 294(14) 5456–5465 **5465**